2940 *Inorg. Chem.* **1989**, *28*, 2940–2944

Contribution from the Department of Chemistry, University of Florence, Florence, Italy, Institut d'Electronique Fondamentale, Orsay, France, and Departement de Recherche Fondamentale, Centre d'Etudes Nucleaires, Grenoble, France

Magnetic Coupling in Zero- and One-Dimensional Magnetic Systems Formed by Nickel(II) and Nitronyl Nitroxides. Magnetic Phase Transition of a Ferrimagnetic Chain

Andrea Caneschi,[1a] Dante Gatteschi,*[,1a] Jean Pierre Renard,[1b] Paul Rey,*[,1c] and Roberta Sessoli[1a]

Received January 9, 1989

Two novel compounds formed by nickel(II) hexafluoroacetylacetonate and nitronyl nitroxide radicals NITR = 2-R-4,4,5,5-tetramethyl-4,5-dihydro-1*H*-imidazole-1-oxyl 3-oxide, with R = methyl, Me, and phenyl, Ph, were synthesized. The compound Ni(hfac)$_2$(NITPh)$_2$ crystallizes in the monoclinic system, space group $P2_1/c$, with a = 12.243 (4) Å, b = 15.237 (4) Å, c = 22.310 (8) Å, β = 100.68 (2)°, and Z = 4. The nickel ions are octahedrally coordinated to two hfac molecules and to the oxygen atoms of two different radicals. The magnetic properties indicate the presence of a strong antiferromagnetic coupling between the nickel and the radicals, which has been roughly estimated to be on the order of 400 cm^{-1}. Even if the structure of Ni(hfac)$_2$NITMe is not available, we suggest an infinite chain structure, with each radical bridging two Ni(hfac)$_2$ units, on the basis of analogies with other M(hfac)$_2$NITR compounds. In agreement with the proposed structure, the magnetic susceptibility shows a divergence in the χT product at low temperature. A numerical fit, with a model previously used for Mn(hfac)$_2$NITR ferrimagnetic chains, yields an antiferromagnetic coupling of 424 cm^{-1}. The fast divergence of the susceptibility at very low temperature indicates the presence of a phase transition to three-dimensional order. Low-field (0–1 Oe) magnetic measurements show that the system undergoes a phase transition at ca. 5.3 K. The nature of the transition is presumably ferromagnetic and is driven by the dipolar interaction between chains, as in the analogous manganese–radical systems.

Introduction

The nitronyl nitroxides NITR = 2-R-4,4,5,5-tetramethyl-4,5-dihydro-1*H*-imidazole-1-oxyl 3-oxide, with R = methyl, ethyl, propyl, and phenyl, have proved to be extremely versatile magnetic ligands, capable of forming one-dimensional magnetic systems with different transition-metal and lanthanide ions.[2–6] In particular we have found that copper(II) hexafluoroacetylacetonate, Cu(hfac)$_2$, forms with NITMe ferromagnetic chains of formula Cu(hfac)$_2$NITMe,[2] while the analogous manganese(II) salts yield ferrimagnetic chains.[3] These compounds have interesting properties, such as apparent spin diffusion effects in the EPR spectra and g shifts determined by short-range order.[2–4,6] The copper derivative does not show any transition to three-dimensional magnetic order down to 1 K,[7] although the magnetic susceptibility data yield some evidence of a weak interchain antiferromagnetic interaction. The manganese(II) compounds on the other hand undergo a transition to three-dimensional ferromagnetic order at ca. 8 K.[4,6]

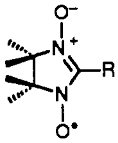

NITR

In view of the current interest in the synthesis of molecular magnets,[8–16] it is important to determine how the nature of the metal ions influences the exchange interactions within the chains and the intermolecular couplings eventually leading to three-dimensional magnetic order. Therefore we decided to study chains formed by nickel(II) and nitronyl nitroxides. Up to now only two well-characterized nickel(II) compounds with nitroxides have been reported, namely Ni(hfac)$_2$(proxyl)$_2$,[17] where proxyl is 2,2,5,5-tetramethylpyrrolinyl-1-oxy, and an adduct of formula [Ni(hfac)$_2$NITEt]$_2$ with the radical bridging to two metal ions.[18] Both compounds show strong antiferromagnetic coupling between the metal ion and the radical (J > 300 cm^{-1}). If a similar interaction operates between nickel ions and nitronyl nitroxides arranged in a chain similar to those observed in copper and manganese M(hfac)$_2$NITR derivatives, the expected magnetic behavior is that of one-dimensional ferrimagnets, which are characterized by large uncompensated moments at low temperatures. It will be interesting therefore to check if the chains order magnetically in three dimensions and to compare the transition temperatures with those of Mn(hfac)$_2$NITR.

We wish to report here the magnetic properties of Ni(hfac)$_2$NITMe, which, although we could not obtain suitable crystals for X-ray analysis, is apparently one-dimensional and behaves as a ferrimagnetic linear chain undergoing a magnetic phase transition at ≅5 K. Further, in order to characterize the nature of exchange between nickel(II) and nitronyl nitroxides, we wish to report here the crystal structure and the magnetic

Table I. Crystallographic Data for Ni(hfac)$_2$(NITPh)$_2$

formula: $NiC_{36}H_{36}F_{12}N_4O_8$	fw = 939.38
a = 12.423 (4) Å	space group: $P2_1/c$ (No 14)
b = 15.237 (4) Å	T = 22 °C
c = 22.310 (8) Å	λ = 0.7107 Å (Mo Kα)
β = 100.68 (2)°	μ = 5.36 cm^{-1}
V = 4150.0 Å^3	R = 0.060
Z = 4	R_w = 0.059
ρ(calcd) = 1.50 g/cm^3	

---

(1) (a) University of Florence. (b) Institut d'Electronique Fondamentale. (c) Centre d'Etudes Nucleaires.

(2) Caneschi, A.; Gatteschi, D.; Laugier, J.; Rey, P. *J. Am. Chem. Soc.* **1987**, *109*, 2191.

(3) Caneschi, A.; Gatteschi, D.; Rey, P.; Sessoli, R. *Inorg. Chem.* **1988**, *27*, 1756.

(4) Caneschi, A.; Gatteschi, D.; Renard, J. P.; Rey, P.; Sessoli, R. *Inorg. Chem.* **1989**, *28*, 1976.

(5) Benelli, C.; Caneschi, A.; Gatteschi, D.; Pardi, L.; Rey, P. *Inorg. Chem.* **1989**, *28*, 275.

(6) Caneschi, A.; Gatteschi, D.; Renard, J. P.; Rey, P.; Sessoli, R. *Inorg. Chem.*, in press.

(7) Unpublished results from our laboratory.

(8) Miller, J. S.; Epstein, A. J.; Reiff, W. M. *Chem. Rev.* **1988**, *88*, 201.

(9) Miller, J. S.; Epstein, A. J.; Reiff, W. M. *Acc. Chem. Res.* **1988**, *21*, 114.

(10) Verdaguer, M.; Julve, M.; Michalowicz, A.; Kahn, O. *Inorg. Chem.* **1983**, *22*, 2624.

(11) Kahn, O. In *Organic and Inorganic Low-Dimensional Crystalline Materials*; Delhaes, P., Drillon, M., Eds.; NATO ASI Series 168; Plenum: New York, 1987.

(12) Korshak, Yu. V.; Medvedeva, T. V.; Ovchinnikov, A. A.; Spector, V. N. *Nature* **1987**, *326*, 370.

(13) Le Page, T. J.; Breslow, R. *J. Am. Chem. Soc.* **1987**, *109*, 6412.

(14) Sugawara, T.; Bandow, S.; Kimura, K.; Iwamura, H.; Itoh, K. *J. Am. Chem. Soc.* **1986**, *108*, 368.

(15) Beltran, D.; Escriva, E.; Drillon, M. *J. Chem. Soc. Faraday Trans.* **1982**, *78*, 1773.

(16) Georges, R.; Curély, J.; Drillon, M. *J. Appl. Phys.* **1985**, *58*, 914.

(17) Porter, L. C.; Dickman, M. H.; Doedens, R. J. *Inorg. Chem.* **1988**, *27*, 1548.

(18) Caneschi, A.; Gatteschi, D.; Laugier, J.; Rey, P.; Sessoli, R. *Inorg. Chem.* **1988**, *27*, 1553.

0020-1669/89/1328-2940$01.50/0

Table II. Positional Parameters ($\times 10^4$) and Thermal Factors ($Å^2 \times 10^3$) for $Ni(hfac)_2(NITPh)_2$[a]

	x	*y*	*z*	$U_{iso/iso_{eq}}$
Ni	2333 (1)	807 (1)	2355 (1)	38
O1	1594 (4)	1660 (3)	2847 (2)	45
O2	3649 (4)	792 (3)	3032 (2)	46
O3	1010 (4)	845 (3)	1692 (2)	48
O4	3056 (4)	−27 (3)	1838 (3)	48
O5	3094 (4)	1917 (3)	2073 (2)	43
O6	3977 (6)	2697 (5)	226 (3)	100
O7	1662 (4)	−330 (3)	2657 (2)	43
O8	1002 (5)	−958 (4)	4581 (3)	70
N1	3059 (5)	2257 (4)	1546 (3)	39 (2)
N2	3464 (6)	2619 (5)	666 (3)	59 (2)
N3	1776 (5)	−630 (4)	3206 (3)	36 (2)
N4	1452 (5)	−924 (4)	4114 (3)	46 (2)
C1	2097 (7)	2119 (5)	3272 (4)	45 (2)
C2	3847 (7)	1373 (5)	3432 (4)	46 (2)
C3	3145 (7)	2029 (5)	3574 (4)	55 (2)
C4	1423 (9)	2877 (7)	3434 (5)	67
C5	5004 (10)	1334 (8)	3792 (5)	76
C6	778 (7)	299 (6)	1273 (4)	49 (2)
C7	2527 (7)	−442 (6)	1402 (4)	50 (2)
C8	1448 (7)	−341 (6)	1110 (4)	59 (3)
C9	−366 (8)	382 (7)	920 (5)	64
C10	3182 (10)	−1167 (8)	1171 (6)	87
C11	3734 (6)	2084 (5)	1157 (4)	46 (2)
C12	2386 (7)	3070 (5)	1366 (4)	47 (2)
C13	2416 (8)	3108 (6)	679 (4)	62 (3)
C14	1252 (6)	2974 (6)	1509 (4)	59
C15	3012 (7)	3813 (6)	1737 (4)	71
C16	1533 (8)	2580 (8)	288 (4)	93
C17	2482 (9)	4017 (7)	414 (5)	107
C18	4624 (4)	1450 (3)	1250 (3)	54 (2)
C19	4988 (4)	1093 (3)	747 (3)	73 (3)
C20	5842 (4)	485 (3)	833 (3)	96 (4)
C21	6332 (4)	233 (3)	1422 (3)	91 (4)
C22	5968 (4)	590 (3)	1925 (3)	89 (4)
C23	5114 (4)	1199 (3)	1839 (3)	60 (3)
C24	1122 (6)	−428 (5)	3603 (3)	39 (2)
C25	2491 (6)	−1414 (5)	3403 (4)	45 (2)
C26	2522 (7)	−1394 (5)	4094 (4)	47 (2)
C27	1870 (7)	−2196 (5)	3068 (4)	70
C28	3596 (7)	−1314 (6)	3212 (4)	64
C29	3403 (7)	−820 (6)	4451 (4)	76
C30	2507 (8)	−2284 (6)	4398 (5)	86
C31	193 (4)	152 (3)	3514 (2)	43 (2)
C32	−378 (4)	300 (3)	2923 (2)	47 (2)
C33	−1286 (4)	855 (3)	2826 (2)	59 (2)
C34	−1623 (4)	1263 (3)	3320 (2)	64 (3)
C35	−1052 (4)	1115 (3)	3911 (2)	71 (3)
C36	−143 (4)	559 (3)	4008 (2)	55 (2)
F1	1941 (6)	3349 (4)	3895 (4)	137
F2	1206 (9)	3434 (5)	3022 (3)	203
F3	583 (6)	2651 (5)	3620 (5)	186
F4	5225 (6)	601 (5)	4068 (5)	187
F5	5294 (5)	1953 (5)	4191 (3)	108
F6	5708 (5)	1419 (7)	3435 (3)	156
F7	−688 (5)	−281 (4)	533 (3)	98
F8	−1102 (4)	441 (5)	1262 (3)	116
F9	−474 (5)	1086 (4)	568 (3)	99
F10	2710 (7)	−1862 (5)	1041 (6)	200
F11	4071 (9)	−1352 (8)	1508 (5)	227
F12	3504 (10)	−972 (7)	690 (5)	229

[a] Standard deviations in the last significant digit are in parentheses.

Table III. Selected Bond Distances (Å) and Angles (deg) in $Ni(hfac)_2(NITPh)_2$[a]

Ni–O1	2.027 (5)	Ni–O2	2.009 (5)
Ni–O3	1.998 (5)	Ni–O4	2.035 (6)
Ni–O5	2.090 (5)	Ni–O7	2.087 (5)
O1–C1	1.249 (9)	O2–C2	1.249 (10)
O3–C6	1.245 (10)	O4–C7	1.240 (10)
O5–N1	1.278 (8)	O6–N2	1.272 (11)
O7–N3	1.291 (8)	O8–N4	1.272 (9)
N1–C11	1.338 (11)	N2–C11	1.356 (11)
N3–C24	1.344 (10)	N4–C24	1.366 (10)
O5–Ni–O7	176.7 (2)	O4–Ni–O7	84.8 (2)
O4–Ni–O5	93.6 (2)	O3–Ni–O7	86.5 (2)
O3–Ni–O5	96.3 (2)	O3–Ni–O4	89.2 (2)
O2–Ni–O7	93.8 (2)	O2–Ni–O5	83.4 (2)
O2–Ni–O4	92.1 (2)	O2–Ni–O3	178.7 (2)
O1–Ni–O7	96.3 (2)	O1–Ni–O5	85.5 (2)
O1–Ni–O4	178.2 (2)	O1–Ni–O3	89.4 (2)
O1–Ni–O2	89.3 (2)	Ni–O5–N1	131.7 (4)
Ni–O7–N3	128.3 (4)		

[a] Standard deviations in the last significant digit are in parentheses.

properties of $Ni(hfac)_2(NITPh)_2$.

Experimental Section

Synthesis of the Complexes. $Ni(hfac)_2 \cdot 2H_2O$ was prepared by mixing a stoichiometric amount of hexafluoroacetylacetone with $Ni(CH_3CO-O)_2 \cdot 4H_2O$ in water. The NITR radicals were prepared as previously described.[19,20]

$Ni(hfac)_2NITMe$. First 0.5 mmol of $Ni(hfac)_2 \cdot 2H_2O$ was dissolved in 50 mL of boiling n-heptane and then the solution was cooled to 80 °C. Then 0.55 mmol of NITMe radical was added and the solution allowed to cool down; after 1 h red-violet thin elongated crystals were collected. The compound analyzed satisfactorily for $Ni(hfac)_2NITMe$. Anal. Calcd for $C_{18}F_{12}H_{17}N_2NiO_6$: C, 33.54; H, 2.64; N, 4.35; Ni, 10.12. Found: C, 33.84; H, 2.72; N, 4.34; Ni, 9.94.

$Ni(hfac)_2(NITPh)_2$. A sample of 0.25 mmol of $Ni(hfac)_2 \cdot 2H_2O$ was dissolved in boiling *n*-heptane and then 0.5 mmol of NITPh was added, and the solution was stored at −15 °C for 24 h. Black crystals were collected, which analyzed satisfactorily for $C_{36}F_{12}H_{36}N_4NiO_8$. Anal. Calcd: C, 46.01; H, 3.83; N, 5.96. Found: C, 45.89; H, 3.83; N, 5.84.

X-ray Data Collection and Structure Solution. Diffraction data for $Ni(hfac)_2(NITPh)_2$ were collected at room temperature with an Enraf Nonius CAD4 four-circle diffractometer equipped with Mo Kα radiation. More details are given in Table SI of the supplementary material of which Table I is an abbreviated form. The data were corrected for Lorentz and polarization effects but not for absorption and extinction. Refined unit cell parameters were determined from the setting angles of 15 machine-centered reflections. The space group $P2_1/c$ was determined by the systematic extinctions. The Patterson map revealed the position of the nickel atom while the other atoms were found by successive difference Fourier syntheses using the SHELX-76 package.[21] Anisotropic thermal factors were introduced for the heavy atom, the oxygen, the fluorine, the carbon atoms of the methyl groups, and those bonded to fluorine. Hydrogen atoms were introduced in fixed and idealized positions with isotropic thermal parameters 20% larger than those of the relative carbon atoms. The main feature of the present structure lay in the disorder and/or thermal motion found in the CF_3 groups. Nevertheless, it did not affect seriously the precision of the structural results, and final least-squares refinements converged at $R = 0.060$ and $R_w = 0.059$. The highest peaks in the last difference Fourier map were on the order of 0.6 e/Å^3 and were situated near the CF_3 groups. Final atomic coordinates for $Ni(hfac)_2(NITPh)_2$ are shown in Table II.

Magnetic Measurements. Magnetic measurements in an applied field in the range 0.01–0.5 T were performed by using an SHE superconducting SQUID magnetometer. Data were corrected for the magnetization of the sample holder and for diamagnetic contributions, which were estimated from Pascal's constants.

Measurements in an external magnetic field ranging between 0 and 0.1 mT were performed with a laboratory-made low-field SQUID magnetometer[22] in the temperature range 2–10 K.

Results

Structure of $Ni(hfac)_2(NITPh)_2$. The nickel atom is bound to two chelating hfac ligands and two nitroxides in a trans-octahedral configuration. A view of the molecular structure is given in Figure 1. Selected bond distances and angles are given in Table III. The bond distances between nickel(II) and the oxygens of the hfac molecules compare well with those reported for other similar complexes,[23,24] and the distances to the oxygen atoms of the NITPh

---

[19] Lamchen, M.; Wittag, T. W. *J. Chem. Soc.* **1966**, 2300.

[20] Ullman, E. F.; Call, L.; Osiecky, J. H. *J. Org. Chem.* **1970**, *35*, 3623.

[21] Sheldrick, G. "SHELX 76 System of Computing Program"; University of Cambridge, Cambridge, England, 1976. Atomic scattering factors were from: Cromer, D. T.; Liberman, D. J. *J. Chem. Phys.* **1970**, *53*, 1891.

[22] Beauvillain, P.; Chappert, C.; Renard, J. P. *J. Phys. E* **1985**, *18*, 839.

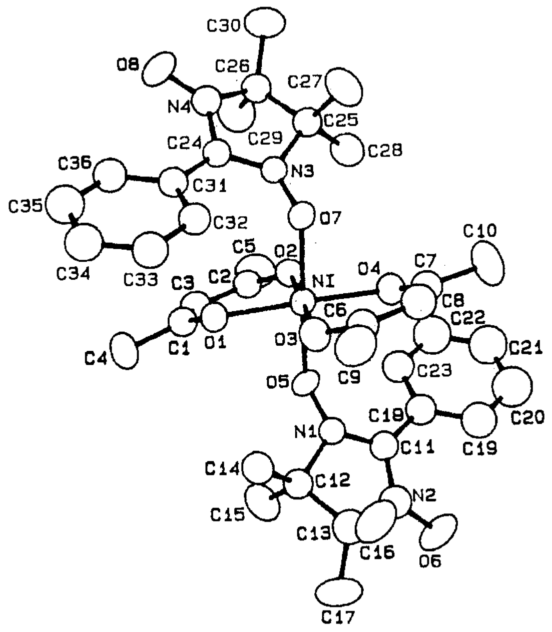

Figure 1. ORTEP view of $Ni(hfac)_2(NITPh)_2$.

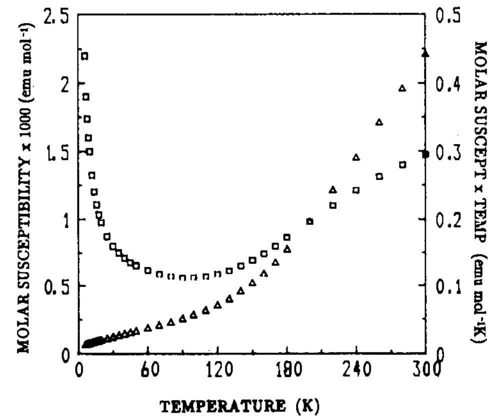

Figure 2. Temperature dependence of the magnetic susceptibility of $Ni(hfac)_2(NITPh)_2$ in the form χ (□) and χT (△) vs temperature.

molecules are only slightly shorter than those reported for the proxyl ligand (2.090 (5) and 2.087 (5) Å vs 2.100 (4) Å).[17] The Ni–O–N angles, which are relevant to the mechanism of exchange between metal ions and nitroxides,[25,26] are 131.7 (4) and 128.3 (4)°, respectively. The planes of the nitroxides are almost orthogonal to the Ni–O–N planes (87.6 (8) and 89.8 (8)°, respectively). The N–O distance of the two coordinated groups are equal within error (1.278 (8) and 1.291 (8) Å), as well as the N–O distances of the two groups (1.272 (11) and 1.272 (9) Å). All these distances are typical for a nitronyl nitroxide radical.[27] The phenyl rings make angles of 24.9 (5) and 27.0 (3)° with the planes of the nitroxides.

No significant intermolecular contacts are observed. The shortest distance between noncoordinated NO groups is 4.46 Å.

Magnetic Data. The temperature dependence of the magnetic susceptibility of $Ni(hfac)_2(NITPh)_2$ in the range 4–300 K measured in an applied field of 0.5 T is shown in Figure 2. The room temperature value of χT, 0.44 emu mol^{-1} K, is much lower than the value expected for uncorrelated spins, indicating that the metal ions and the nitroxides are strongly coupled in an antiferromagnetic fashion. χT decreases smoothly with decreasing temperature, and below 120 K, the compound becomes practically diamagnetic, except for the presence of a paramagnetic impurity as shown by the χ vs T curve, which decreases with decreasing temperature in the range 300–90 K and then increases.

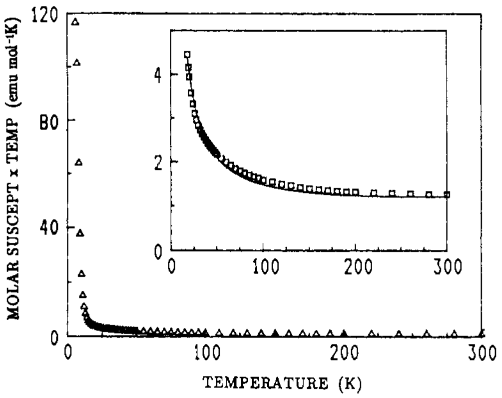

Figure 3. χT vs temperature of $Ni(hfac)_2NITMe$. In the inset the solid line is calculated as described in the text with $J = 424$ cm^{-1} and $g_{Ni} = 2.3$.

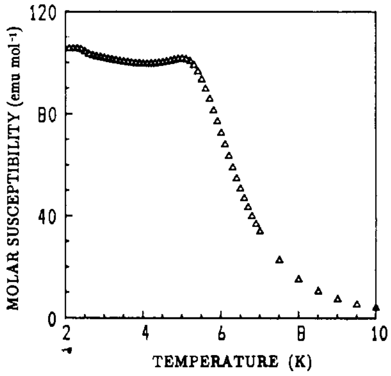

Figure 4. Magnetic susceptibility per mole of $Ni(hfac)_2NITMe$ measured in an external magnetic field of 1 Oe.

A detailed analysis of the experimental data cannot be performed, because the available range of temperatures at which the χT product is significantly different from zero is rather narrow; however, the value of J can be approximately estimated to be close to 400 cm^{-1}. We use the spin-Hamiltonian in the form $H = JS_1S_2$, and a positive J corresponds to antiferromagnetic coupling.

The temperature dependence of the magnetic susceptibility of $Ni(hfac)_2NITMe$ is shown in Figure 3. The χT vs T curve increases steadily with decreasing temperature, starting from a room-temperature value of 1.26 emu mol^{-1} K, which is lower than the value expected for uncorrelated spins. Below 20 K the curve takes off reaching a value of 130 emu mol^{-1} K at 4 K in a field of 10 mT, indicating that the system is an extended one. In fact such high values can be observed for either a ferro- or a ferrimagnetic one-dimensional system, in which χT is expected to diverge at low temperature.[28] The fast increase in χT below 10 K may be indicative of a magnetic phase transition; therefore, we performed experiments in low fields. The magnetization of a polycrystalline sample in a field of 0.1 mT is shown in Figure 4. These data clearly show a magnetic phase transition at ca. 5.3 K. The rounded maximum observed at 5 K is typical of measurements performed on polycrystalline samples, because, while the crystallites with the easy axis parallel to the field are expected to give a contribution that is temperature independent, those with the intermediate and hard axes are expected to decrease on lowering the temperature. Below 4.5 K, the magnetization curve increases with decreasing temperature, probably due to irreversibility factors in the movements of the domain walls.

---

(23) Montgomery, H.; Lingafelter, E. C. *Acta Crystallogr.* **1964**, *17*, 1481.

(24) Cramer, R. E.; Cramer, S. W.; Cramer, K. F.; Chudyk, M. A.; Seff, K. *Inorg. Chem.* **1977**, *16*, 219.

(25) Caneschi, A.; Gatteschi, D.; Grand, A.; Laugier, J.; Pardi, L.; Rey, P. *Inorg. Chem.* **1988**, *27*, 1031.

(26) Caneschi, A.; Gatteschi, D.; Laugier, J.; Pardi, L.; Rey, P.; Zanchini, C. *Inorg. Chem.* **1988**, *27*, 2027.

(27) Wong, W. H.; Watkins, S. F. *J. Chem. Soc., Chem. Commun.* **1973**, 888.

(28) Verdaguer, M.; Gleizes, A.; Renard, J. P.; Seiden, J. *Phys. Rev. B* **1984**, *29*, 5144.

In order to characterize the nature of the phase transition, the magnetization has been measured at 5 K in three different magnetic fields: 55, 100, and 200 mT. The values of the magnetization are 1700, 3646, and 4044 emu mol^{-1} G, respectively.

Discussion

The stoichiometry and the magnetic properties of Ni($hfac)_2NITMe$ are clearly indicative of a linear-chain structure, similar to that reported for analogous copper(II)[2] and manganese(II)[3] compounds. The suggested coordination around nickel(II) is octahedral, presumably similar to that observed in Ni($hfac)_2(NITPh)_2$,[17] although we cannot exclude that the bridging nitroxides coordinate cis rather than trans around the metal ion. A similar alternation of cis and trans coordination was observed in various manganese derivatives.[3,6,29] In the present compound, the nitronyl nitroxide is bonded with the two oxygen atoms to two different nickel ions:

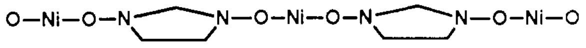

From the magnetic point of view, this leaves two possibilities open, i.e., either a one-dimensional ferromagnet or ferrimagnet, according to the nature of the exchange interaction between the metal and the radical. In a qualitative way the two different types of behavior can be discriminated in the paramagnetic region, where a ferromagnetic chain is expected to have χT steadily increasing with decreasing temperature, while for a ferrimagnetic chain χT initially decreases with decreasing temperature, reaches a minimum that is expected to fall in the temperature range 0.4–0.6 J/K, depending on the model,[10,30,31] and then increases on decreasing temperature as a consequence of the short range that keeps the uncompensated magnetic moments parallel to each other. Both types of chains have of course the same high-temperature limit of χT, corresponding to the uncorrelated spins. For a nickel–radical chain this value can be estimated to be 1.4–1.6 emu mol^{-1} K, the uncertainty being determined by the g value of nickel(II).

In the present case, χT keeps increasing with decreasing temperature over the whole investigated range, so that a ferromagnetic chain might be a suitable candidate to interpret the data. However the room-temperature χT value is significantly lower than expected for uncorrelated spins; therefore, it is more satisfactory to consider Ni($hfac)_2NITMe$ as a ferrimagnetic chain with $J > 350$ cm^{-1} in such a way that the experimental curve below 300 K corresponds to the region below the minimum.

A confirmation to this interpretation comes from the analysis of the magnetic data of Ni($hfac)_2(NITPh)_2$, which shows that the coupling between the metal ion and the radical is antiferromagnetic, with $J \cong 400$ cm^{-1}. Similar results were previously reported for Ni($hfac)_2(proxyl)_2$.[17] The origin of this relatively strong antiferromagnetic coupling between nickel(II) and radical is easily understood on the basis of a simple orbital model analogous to that which has been previously used to interpret the magnetic properties of copper(II) and manganese(II) complexes.[25,26] In fact for an octahedral nickel(II) complex the magnetic orbitals are d_{z^2} and $d_{x^2-y^2}$, and the observed coupling constant can be decomposed into the sum of two contributions according to

$$J = \tfrac{1}{2}(J_{z^2-\pi^*} + J_{x^2-y^2-\pi^*}) \qquad (1)$$

where the J_{ik} constants are the isotropic coupling constants between the indicated metal orbitals and the π^* magnetic orbital of the radical.

For the observed geometries the overlap between $x^2 - y^2$ and π^* is essentially zero, and the corresponding J_{ik} is expected to be weak ferromagnetic, as observed in a series of tetragonal copper(II)–nitroxide complexes.[25] The overlap between z^2 and π^* on the other hand is significantly different from zero as soon as the Ni–O–N angle is lower than 180° and the angle between the plane of the radical and the Ni–O–N plane is close to 90°, as is observed in the structure of both Ni($hfac)_2(NITPh)_2$ and Ni($hfac)_2(proxyl)_2$. A large overlap between the magnetic orbitals indicates strong antiferromagnetic coupling; therefore, we may safely anticipate large positive J values for both the mononuclear complexes, as experimentally observed.

A comparison of the crystal structures of Ni($hfac)_2(proxyl)_2$ and Ni($hfac)_2(NITPh)_2$ shows that as far as the geometrical parameters are concerned the overlap between the magnetic orbitals should be larger for the latter; therefore, the observed larger coupling constant for the former must be justified on the basis of an intrinsic larger overlap of the nitroxide compared to the nitronyl nitroxide. Similar conclusions were previously reached for manganese(II) complexes.[3]

With these considerations in mind, the χT vs T curve of Ni($hfac)_2(NITMe)$ was fitted by assuming an antiferromagnetic coupling between the metal ion and the radical. Several approximate treatments are available for ferrimagnetic chains, which treat either all the spins as classical spins[30] or alternatively the spins $S = {}^1/_2$ as quantum spins and the others as classical spins.[31] Both methods are not totally satisfactory in the present case where the $S = 1$ spins are fairly distant from the classical limit; however, we are forced to use them due to the lack of more accurate treatments.

The best fit of the experimental points with the quantum–classical[3,31] expression is shown in Figure 3. The agreement can be considered as satisfactory. The present model does not reproduce the behavior at very low temperature due to the occurrence of the phase transition. The calculated value of J (424 cm^{-1}) is close to that obtained for Ni($hfac)_2(NITPh)_2$.

The relatively large value of J has the consequence to determine a fairly strong spin correlation at low temperature. The determination of the correlation length is not simple, but in the present case it is possible to use simplified arguments in order to arrive at a reasonable guess.[6] In fact below 100 K, we can safely assume that isolated nickel–nitroxide pairs would be in the ground state with $S = {}^1/_2$, and the average correlation length at low temperature is then estimated by comparing the observed χT value for a nickel–radical unit in Ni($hfac)_2NITMe$ with that of a system with $S = {}^1/_2$. For instance, we found that at 15 K the correlation length corresponds to about 37 nickel–radical units, i.e. the average length of segments in which all the spins $S = 1$ are, for example, up, and the spins $S = {}^1/_2$ are down. Although in a one-dimensional system long-range order can be established only at 0 K,[32] the relatively large effective spins that are created by short-range order can make the interactions between chains relatively strong and therefore determine transitions to three-dimensional magnetic order. This has indeed been found to be the case for Mn($hfac)_2$NITi-Pr,[5] Mn($hfac)_2$NITEt, and Mn($hfac)_2$NITn-Pr,[6] which undergo a ferromagnetic phase transition at 7.6, 8.1, and 8.6 K respectively. Since the chains are well shielded and no obvious exchange pathway is available, we assumed that the driving force to three-dimensional order was the dipolar interaction between chains, and this was confirmed by approximate calculations.

In the present case, the nature of the magnetic phase transition is not univocally determined by our measurements on polycrystalline powders. In fact the observed spontaneous magnetization might originate from either a parallel or an antiparallel alignment of the spins of the chains. In the latter case a canting of the spins would be needed to justify the observed magnetization, and this, in turn, should be determined by crystal field anisotropy of the nickel ions.[33] However the value of the magnetization reached in a relatively low magnetic field seems to indicate a ferromagnetic nature of the transition. In fact the ordered state corresponds to that of a ferrimagnet formed by the sublattice of the spins $S = {}^1/_2$ of the radicals and that of the spins $S = 1$ of the nickel ions yielding a saturation magnetization of 6143 emu mol^{-1} G for $g_{Ni} = 2.2$. In a magnetic field of 55 mT, only the crystallites with the easy axis parallel to the applied field are expected to reach

---

(29) Caneschi, A.; Gatteschi, D.; Laugier, J.; Rey, P.; Sessoli, R.; Zanchini, C. *J. Am. Chem. Soc.* **1988**, *110*, 2795.

(30) Drillon, M.; Coronado, E.; Beltran, D.; Georges, R. *Chem. Phys.* **1983**, *79*, 449.

(31) Seiden, J. *J. Phys., Lett.* **1983**, *44*, L947.

(32) Stanley, H. E. *Introduction to Phase Transitions and Critical Phenomena*; Clarendon Press: Oxford, England, 1971.

(33) Moriya, T. *Phys. Rev.* **1960**, *117*, 635.

the saturation, and a magnetization value of 1700 emu mol^{-1} G, as experimentally observed, seems to be in good agreement with our hypothesis.

We assume that the dipolar interaction between the chains is the driving force to three-dimensional ferromagnetic order also in Ni(hfac)$_2$NITMe. Qualitatively, the lower transition temperature, compared with the manganese chains, can be explained by the smaller spin of nickel(II) compared to manganese(II), which makes the dipolar interaction less effective. This is also in line with the fact that the analogous copper chain, in which the coupling is much smaller than in the manganese and nickel derivatives and the spin is smaller too, do not undergo any phase transition above 1 K.

In conclusion, in the M(hfac)$_2$NITR magnetic materials the one-dimensional character is very well preserved by the bulky hfac ligands, which do not provide effective exchange pathways between the metal ions. The strong intrachain antiferromagnetic interactions in the manganese and nickel derivatives build up large uncompensated moments at low temperature in such a way that even the weak interchain dipolar interaction is sufficient to establish three-dimensional order. Therefore the transition temperature could in principle be increased by either increasing the intrachain interaction or decreasing the interchain distance. Increasing the intrachain interaction does not seem to be very probable, because studies on model mononuclear complexes show that J of about 300–400 cm^{-1} is the upper limit, while the interchain interaction can be improved by changing the hfac ligands with others that can transmit more efficiently the exchange interaction. Indeed, we found that [Mn(pfb)$_2$]$_2$NITR, where pfb is pentafluorobenzoate, orders three-dimensionally above 20 K.[34]

Acknowledgment. The financial support of the Italian Ministry of Public Education and of the CNR is gratefully acknowledged.

Registry No. Ni(hfac)$_2$NITMe, 121269-34-9; Ni(hfac)$_2$(NITPh)$_2$, 121288-63-9; Ni(hfac)$_2$, 14949-69-0.

Supplementary Material Available: Table SI, listing crystallographic data, Tables SII–SV, listing anisotropic thermal factors, bond distances, bond angles, and calculated positional parameters of hydrogen atoms, and Table SVI, listing least-squares planes and deviations (12 pages); tables of calculated and observed structure factors (14 pages). Ordering information is given on any current masthead page.

---

(34) Caneschi, A.; Gatteschi, D.; Renard, J. P.; Rey, P.; Sessoli, R. *J. Am. Chem. Soc.* **1989**, *111*, 785.

Contribution from the Dipartimento di Chimica Inorganica e Struttura Molecolare, Università di Messina, Salita Sperone, 31, Villaggio S. Agata, I-98100 Messina, Italy, and Dipartimento di Chimica Inorganica, Chimica Fisica e Chimica dei Materiali, Università di Torino, Via P. Giuria, 7, I-10125 Torino, Italy

Bi- and Polynuclear Complexes with Short-Bite Ligands Bridging Metal Atoms. [(η^5-C$_5$H$_5$)Rh(μ-CH$_3$O$_2$CC$_2$CO$_2$CH$_3$)(μ-Ph$_2$Ppy)Rh(CO)(μ-Cl)]$_2$: Synthesis, X-ray Crystal Structure, Structural Dynamics, and Reactions with CO and SO$_2$

Enrico Rotondo,[1a] Sandra Lo Schiavo,[1a] Giuseppe Bruno,[1a] Carmela Grazia Arena,[1a] Roberto Gobetto,[1b] and Felice Faraone*,[1a]

Received November 28, 1988

Treatment of [(η^5-C$_5$H$_5$)Rh(μ-CO)(μ-Ph$_2$Ppy)Rh(CO)Cl] (1) (Ph$_2$Ppy = 2-(diphenylphosphino)pyridine) with the activated acetylenes dimethyl acetylenedicarboxylate (DMA) and diethyl acetylenedicarboxylate (DEA), in CH$_2$Cl$_2$ solution, yields the tetranuclear complexes {[(η^5-C$_5$H$_5$)Rh(μ-DMA)(μ-Ph$_2$Ppy)Rh(CO)(μ-Cl)]$_2$·CH$_2$Cl$_2$} (2) and {[(η^5-C$_5$H$_5$)Rh(μ-DEA)(μ-Ph$_2$Ppy)Rh(CO)(μ-Cl)]$_2$·CH$_2$Cl$_2$} (3), respectively. The alkyne in both the complexes adopts the μ-η^2-$\|$ (cis-dimetalated olefinic) bonding mode. The structure of 2 was established by X-ray crystallography: the crystals are triclinic, space group $P\bar{1}$, with a = 11.805 (1) Å, b = 11.791 (1) Å, c = 12.042 (2) Å, α = 98.7 (2)°, β = 108.9 (2)°, γ = 90.2 (2)°, and Z = 2. Least-squares refinement of 381 parameters using 3971 reflections yields R = 0.035 and R_w = 0.036. The molecule shows a crystallographic inversion center originating from the presence of two asymmetrical bridging chloro ligands that link two bimetallic units. Each rhodium dimer unit is completely asymmetrical and consists of two rhodium atoms bridged by the Ph$_2$Ppy and the DMA ligands. The Rh(1)–Rh(2) bond distance is 2.661 (1) Å and the Rh(1)···Rh(1′) separation is 3.900 (1) Å. The structural parameters concerning the inner coordination sphere provide useful information about the formation of the tetranuclear species 2. Both Rh–Cl distances are somewhat long [Rh(1)–Cl(1) = 2.516 (1) Å, and Rh(1)–Cl(1′) = 2.670 (1) Å]. DMA is attached essentially parallel to the Rh(1)–Rh(2) axis in a cis-dimetalated olefinic geometry; the Rh(1)–C(24) and Rh(2)–C(25) bond distances are significantly different (2.022 (5) and 2.040 (4) Å, respectively). ^{31}P{^{1}H} and ^{1}H NMR spectra of 2 in CD$_2$Cl$_2$ solution, at different temperatures, indicate the presence of an equilibrium between the tetranuclear, 2, and the binuclear, [(η^5-C$_5$H$_5$)Rh(μ-DMA)(μ-Ph$_2$Ppy)Rh(CO)(Cl)] (4), species. The unsaturation of the rhodium(II), 16-electron center in 4 seems to be the key to the reactivity of this species, and it accounts for both the formation of the tetranuclear chloro-bridged species 2 and the reactions of 2 with small molecules such as CO and SO$_2$. The reaction of 2 with CO and SO$_2$ leads to adducts that could not be isolated owing to the reversibility of the process. ^{31}P, ^{1}H, and ^{13}C NMR spectra indicate that in these adducts CO and SO$_2$ are both terminally bonded to rhodium. Hints of a dynamic process involving the formation of acyl derivatives, presumably by insertion of ^{13}CO into the Rh–C(acetylene) bond, are also reported.

Introduction

Previous papers from our laboratories have described the synthesis, and the molecular structure of the symmetric binuclear (η^5-cyclopentadienyl)rhodium complex [Rh$_2$(η^5-C$_5$H$_5$)$_2$(μ-CO)(μ-dppm)] (dppm = bis(diphenylphosphino)methane) characterized by the presence of the short-bite dppm as a bridging ligand.[2] This complex contains an electron-rich rhodium–rhodium bond as evidenced by the reactions with H$^+$, HgCl$_2$, and group 11 atom electrophiles;[3–7] conversely, it does not react with acetylenes, dienes, or alkyl halides. In light of these results and as a part of our interest in the activation of small molecules by bimetallic com-

---

(1) (a) Università di Messina. (b) Università di Torino.

(2) Faraone, F.; Bruno, G.; Lo Schiavo, S.; Bombieri, G. *J. Chem. Soc., Dalton Trans.* **1984**, 533.

(3) Faraone, F.; Lo Schiavo, S.; Bruno, G.; Bombieri, G. *J. Chem. Soc., Chem. Commun.* **1984**, 6.

(4) Bruno, G.; Lo Schiavo, S.; Piraino, P.; Faraone, F. *Organometallics* **1985**, *4*, 1098.

(5) Lo Schiavo, S.; Bruno, G.; Nicolò, F.; Piraino, P.; Faraone, F. *Organometallics* **1985**, *4*, 2091.

(6) Lo Schiavo, S.; Bruno, G.; Piraino, P.; Faraone, F. *Organometallics* **1986**, *5*, 1400.

(7) Bruno, G.; Lo Schiavo, S.; Rotondo, E.; Piraino, P.; Faraone, F. *Organometallics* **1987**, *6*, 2502.

0020-1669/89/1328-2944$01.50/0